



# Rhamonolipids produced by *Pseudomonas aeruginosa* promotes methane hydrates formation in fixed bed silica gel medium

Amit Arora<sup>1,2</sup> · Swaranjit Singh Cameotra<sup>3,4</sup> · Chandrajit Balomajumder<sup>1</sup> · Rajnish Kumar<sup>5</sup> · Anil Kumar Singh<sup>3,6</sup> · B. Santhakumari<sup>7</sup> · Pushpendra Kumar<sup>8</sup> · Sukumar Laik<sup>9</sup>

Received: 25 May 2020 / Accepted: 29 December 2020 / Published online: 30 January 2021  
© The Author(s), under exclusive licence to Springer Nature B.V. part of Springer Nature 2021

## Abstract

Natural gas hydrates are seen as an alternative future energy source. They have also been valued for their carbon dioxide capturing capability, gas separation, desalination, natural gas storage and transportation. Developing economical and viable gas hydrate based technology is one of the most promising research areas of present decade. Successful commercialization of gas hydrate based technology is often curtailed due to slow formation rate. The present study evaluates biosurfactant as a kinetic promoter of methane hydrates formation in a fixed bed C type silica gel medium. Biosurfactant was produced by growing *Pseudomonas aeruginosa* strain A11 in glycerol supplemented mineral salt medium. Biosurfactant characterization with FTIR, NMR and MALDI-TOF spectroscopy revealed it to be a glycolipids type biosurfactant namely rhamnolipids. Saturating C type silica gel with of 100 ppm rhamnolipids solution enhanced the rate of methane hydrates formation by reducing the induction time. Mole of methane consumed and percentage of water to hydrate conversion was observed to be more in 1000 ppm rhamnolipids saturated C type silica gel as compared to quiescent water system and water saturated silica gel system. Overall results suggest that rhamonolipids produced by strain A11 in combination with silica gel can be utilized as environmentally safe kinetic promoter for methane hydrate formation.

**Keywords** Biosurfactant · Glycolipids · Kinetic promoter · Induction time · Energy

## Introduction

Global energy demand has been increasing continuously on the ground of industrialization, urbanization and population explosion. Currently energy demand is largely fulfilled by fossil fuel. In recent years the need for a new and sustainable energy source is being felt owing to limited fossil fuel

resources and environmental concerns. Natural gas hydrates are seen as a promising future energy source (Zhang et al. 2012). Natural gas hydrates are vastly present in permafrost regions and near-coastal seabed (Chong et al. 2016). Methane hydrates are most commonly encountered natural gas hydrates (Chong et al. 2016). Natural gas hydrates are non-stoichiometric compound composed of small gas molecules

✉ Amit Arora  
aroraamitlse@yahoo.com

<sup>1</sup> Department of Chemical Engineering, Indian Institute of Technology Roorkee, Roorkee, Uttarakhand 247667, India

<sup>2</sup> Present Address: Department of Chemical Engineering, Shaheed Bhagat Singh State Technical Campus, Ferozpur, Punjab 152004, India

<sup>3</sup> Institute of Microbial Technology, Chandigarh 160036, India

<sup>4</sup> Present Address: House No. 1103, Sector-11C, Chandigarh 160011, India

<sup>5</sup> Department of Chemical Engineering, Indian Institute of Technology Madras, Chennai 600036, India

<sup>6</sup> Present Address: Sant Baba Bhag Singh University, Khiala, Punjab 147001, India

<sup>7</sup> Centre for Material Characterization, National Chemical Laboratory, Pune 411008, India

<sup>8</sup> Gas Hydrate Research & Technology Centre, Oil and Natural Gas Corporation Ltd (ONGC) ONGC, Complex Phase-II, Panvel, Navi Mumbai 410221, India

<sup>9</sup> Department of Petroleum Engineering, Indian Institute of Technology (Indian School of Mines), Dhanbad 826004, India

occluded in crystalline cells of water molecules (Sloan and Koh 2008). The crystalline structure of solid gas hydrate is formed when water and natural gas are exposed to low temperature and high pressure (Sloan and Koh 2008; Hester and Brewer 2009). Natural gas hydrates based technologies have also been reported to carry out separation of gases, capture of carbon dioxide, desalination, storage and transportation of natural gases.

Extensive utilization of natural gas hydrates has been restricted due to slow formation rate (Arora et al. 2016a, b; Abedi-Farizhendi et al. 2019). The main problem that limits formation rate is inadequate interfacial interaction between gas and water molecule (Meleshkin et al. 2020; Zhang et al. 2020). Interfacial interaction between liquid water (or solid ice) and gas can be improved by several methods such as the application of high pressure (Ruffine et al. 2010), vigorous mixing (Linga et al. 2010), use of surface-active agents (Zhang et al. 2020; Zhong and Rogers 2000; Saw et al. 2014; Chaturvedi et al. 2018) and support systems (Abedi-Farizhendi et al. 2019; Linga et al. 2012; Kumar et al. 2016). Combination of surfactant as well as biosurfactants and support system is considered superior to agitation as no energy is required for enhancing hydrate formation rate (Wang et al. 2012; Heydari and Peyvandi 2019). Surfactants such as Sodium Dodecyl Sulfate (SDS), Tergitol (Zhong and Rogers 2000; Saw et al. 2014), sodium methyl ester sulfonate (SMES) (Chaturvedi et al. 2018) etc. and support systems like silica, sand, bentonite clay, carbon nanostructures (Abedi-Farizhendi et al. 2019; Linga et al. 2012; Kumar et al. 2016) have been used for promoting gas hydrate formation.

In recent years, replacing synthetic surfactants with surfactants of biological origin is advocated as a future of several industrial processes (Arora et al. 2014). Most of the synthetic surfactants have slow degradation rate in natural environment. Few synthetic surfactants produce toxic degradation intermediates that can be harmful for living organisms. Contrary, surfactants of biological origin are environmentally compatible, biodegradable, low toxic and effective even at extreme environmental conditions (Muller et al. 2012). Biological surfactants have potential to replace synthetic surfactants in terms of performance and economic viability (Jiang et al. 2020; Varjani and Upasani 2017).

Biosurfactants are diverse group of extracellular amphiphilic molecules produced by a wide variety of microorganisms (Varjani and Upasani 2017). In recent past, increased demand for environment friendly processes and products, implementation of stringent environmental laws and advancement in biotechnology has drawn the attention of researchers and policy-makers towards biosurfactants (Muller et al. 2012). Biosurfactants have been used successfully for enhancing the gas hydrate formation kinetics (Arora et al. 2016a, b; Jadav et al. 2017). However, combination of

biosurfactant and porous medium for enhancing gas hydrate formation kinetics is rarely reported in literature (Arora et al. 2016a). This restricts our understanding of biosurfactant and porous medium as a gas hydrate promoter (Arora et al. 2016a).

The objective of the present work is to improve the kinetics of methane hydrate formation in porous medium containing glycolipid type biosurfactant solution. Study compares the methane hydrate formation kinetics in porous medium saturated with different concentrations of biosurfactant solution and quiescent water system. The present study reports induction time, moles of gas consumed and percentage water to hydrate conversion.

## Materials and methods

### Biosurfactant production and purification

The biosurfactant producer *Pseudomonas aeruginosa* strain A11 is a rhizospheric bacterium (Singh and Cameotra 2013). Strain A11 was grown on earlier reported minimal salt medium (Arora et al. 2016a). Biosurfactant produced by strain A11 was purified by earlier reported method (Arora et al. 2016a; Singh and Cameotra 2013).

### Biosurfactant characterization

#### Thin layer chromatography (TLC)

Initial characterization of biosurfactant was performed by TLC Silica gel 60 F254 plate (Merck Darmstadt Germany). Mobile phase consisted of chloroform (65): methanol (25): water (4). The solution consisting of glacial acetic acid–sulfuric acid–anisaldehyde in the ratio of 50:1:0.05 was sprayed for developing plates. After spraying, plates were heated at 90 °C for 10 min to detect glycolipids.

#### Fourier transform infrared (FTIR) spectroscopy

The FTIR analysis was performed by Nicolet 6700 FT-IR spectrometer (Thermo Fisher Scientific USA) in KBr pellet. The purified and lyophilized biosurfactant was mixed with 80 mg of spectral-grade KBr (Merck, Germany). The mixture was pressed into pellets with the help of a hydraulic press. The traces of carbon dioxide were removed before spectral measurements by dry nitrogen purging. The spectral measurements were performed in the transmittance mode. The spectra were obtained over the range of 500–4000  $\text{cm}^{-1}$  with the resolution of 4  $\text{cm}^{-1}$ . All data were corrected for background spectrum.

## Nuclear magnetic resonance (NMR)

Both  $^1\text{H}$  NMR and  $^{13}\text{C}$  NMR spectra of purified biosurfactant were acquired in  $\text{CdCl}_2$  with a NMR Bruker Instrument 500 MHz Bruker Advance 600 Germany.

## Matrix-assisted laser desorption/ionization time of flight (MALDI-TOF)

MALDI-TOF mass spectrometry of purified biosurfactant was performed with the MALDI TOF/TOF MS 5800 System (AB Sciex MA, USA). Alpha cyano 4-hydroxy cinnamic acid ( $\alpha$ -CHCA) was used as MALDI matrix. A 10 mg/ml  $\alpha$ -CHCA solution was prepared in 1:1 (v/v) acetonitrile–0.1% trifluoroacetic acid. Biosurfactant solution (1 mg/ml) prepared in methanol was mixed with matrix solution in the ratio of 1:5. From this mixture 0.5  $\mu\text{l}$  of sample solution containing nearly 0.83  $\mu\text{g}$  of rhamnolipids was spotted on to the pre-cleaned 384 wells MALDI plate and dried at room temperature. Samples were then analyzed in positive ion reflectron mode. The equipment has Nd-YAG 355 nm laser with 1000 Hz laser speed and delayed extraction source. The laser energy (8–12  $\mu\text{J}$ ) was optimized to achieve a good signal to noise ratio and extraction delay time was set at 180 ns. Acquisition mass range was 100–1000 Da. The data was acquired using TOF/TOF series explorer software and processed by Data Explorer Software.

## Surface tension and critical micelle concentration (CMC)

The surface tension reducing ability of biosurfactant was determined at 25 °C by a du Nouy tensiometer (CSC Scientific Company Inc. USA) via ring detachment method. The CMC was obtained following serial dilution method given by Singh and Cameotra (2013).

## Hydrate formation

### C-type of silica gel bed preparation

Silica gel used in the present study has (BET) surface area of 540.06  $\text{m}^2/\text{g}$ , specific pore volume of 0.9  $\text{cm}^3/\text{g}$ , average pore diameter of 64 Å and pore diameter of 49.1 Å (Arora et al. 2016a). Fixed bed of 2.5 cm height was prepared by 64.7 g of C type silica. The silica bed was 90% saturate by 52.41 ml of water (Arora et al. 2016a). The volume of water required for complete saturation of the bed was calculated based on the pore volume of the silica gel (Arora et al. 2016a).

## Apparatus and hydrate formation procedure

The schematic diagram of the overall experimental setup showing gas hydrate autoclave apparatus is shown in Supplementary figure (SI) and its description is given in earlier work (Arora et al. 2016a). Data acquisition was done with inbuilt software. Initially, the experimental runs were performed in quiescent water system, then experimental runs were performed in fixed bed system of C type of silica gel saturated (90%) at various dosage of rhamnolipids solution and with water alone for methane hydrate formation. Kinetic experiments were performed to determine induction time, moles of gas consumed and total water to hydrate conversion (Arora et al. 2016a).

## Scanning electron microscopy (SEM)

For visualizing the morphological changes induced in C type silica gel before and after gas hydrate formation, SEM analysis was performed using Hitachi S-3400N SEM (HITACHI, Japan). The powder samples were coated with gold by plasma prior to measurement.

## Data analysis

Data obtained during kinetic studies were used for determining induction time, moles of gas consumed during methane hydrate formation and percentage water to hydrate conversion following earlier reported formulas (Arora et al. 2016a).

### Total number of moles consumed

The following equations were used for calculating the number of moles of methane gas consumed during hydrate formation

$$(\Delta n_{\text{H}_2})_t = V_{\text{CR}}(P/zRT)_0 - V_{\text{CR}}(P/zRT)_t \quad (1)$$

$$Z = 1 + \beta^0 (P_r/T_r) + w\beta^1 (P_r/T_r) \quad (2)$$

$$\text{Where } \beta^0 = 0.083 - (0.422/T_r^{1.6}) \quad \beta^1 = 0.139 - (0.172/T_r^{4.2})$$

$$T_r = (T_{\text{exp}}/T_{\text{critical}}) \quad P_r = (P_{\text{exp}}/P_{\text{critical}}) \quad w = \text{Acentric factor}$$

where  $z$  is the compressibility factor computed using Pitzer's equation with help of gas uptake data and it varies as the reaction proceeds.

$V_{\text{CR}}$  = Volume of methane gas present in the crystallizer.

$T$  and  $P$  represent temperature and pressure of the crystallizer at different time instants.

## Calculation of the water to hydrate conversion

The amount of water which gets converted to hydrate was calculated with help of following equation (Linga et al. 2010):

$$\text{Conversion of water to hydrate (mol\%)} = \frac{\Delta n_{H,\downarrow} \times \text{Hydration No.}}{n_{H_2O}} \times 100 \quad (3)$$

where  $\Delta n_{H,\downarrow}$  is the total number of moles of gas utilized till the end of the hydrate formation process as determined from the gas uptake measurements and  $n_{H_2O}$  is the total number of moles of water in the system. The hydration number used for the above calculations is 5.75 (Sloan and Koh 2008).

## Results and discussion

### Biosurfactant production by *Pseudomonas aeruginosa* strain A11

Rhamnolipids is one of the well studied microbial surfactant. Muller et al. (2012) proposed rhamnolipids as a next generation surfactant owing to its well documented potential to replace synthetic surfactants. Rhamnolipids is produced by *Pseudomonas aeruginosa* and several related species as a mixture of congeners and homologues (Muller et al. 2012; Varjani and Upasani 2017). Variation reported in rhamnolipids composition is mainly related to strain, growth conditions and growth media composition (Muller et al. 2012; Varjani and Upasani 2017; Singh and Cameotra 2013).

The *P. aeruginosa* strain A11 is well known biosurfactant producer (Arora et al. 2016a; Singh and Cameotra 2013). Strain A11 can produce biosurfactant while growing on diverse group of water-soluble and water-insoluble substances (Singh and Cameotra 2013). In the present study, strain A11 was given 4% (v/v) glycerol as a source of carbon and energy. As evident from Fig. 1a, strain A11 decreased

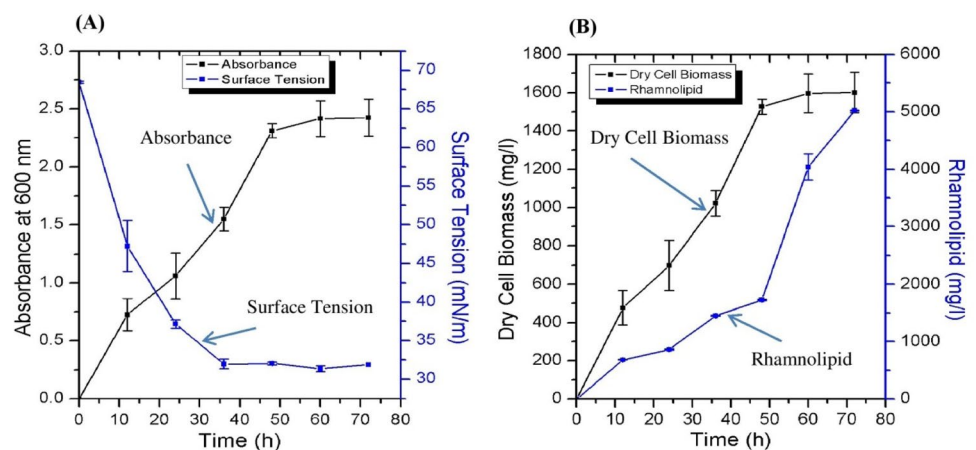
the surface tension significantly more than 50% of growth medium with in 36 h of growth indicating production of biosurfactant. As evident from fig 1b after 72 h of growth, strain A11 produced 5000 mg/l of biosurfactant (Arora et al. 2016a).

Cost of carbon source adds major portion towards the biosurfactant production cost (Jiang et al. 2020). Use of low-cost renewable carbon source such as agro-industrial by-products can make biosurfactant production more economically viable (Jiang et al. 2020). Glycerol is a byproduct of biodiesel and several other oleochemicals production processes (Sun and Chen 2008). Glycerol along with glucose is most widely reported water-soluble carbon source for biosurfactant production (Jiang et al. 2020). Rhamnolipids production on glycerol based growth medium has been reported to reduce the cost of biosurfactant production (Muller et al. 2012; Jiang et al. 2020; Singh and Cameotra 2013). Earlier study considered 3% (v/v) glycerol as most optimum concentration for biosurfactant production (Singh and Cameotra 2013). However, in the present study, glycerol concentration of 4% (v/v) along with trace element solution was found to be optimum for the biosurfactant production. Wu et al. (2008) reported that *P. aeruginosa* EM1 can produce 4.93 g/l of rhamnolipids while growing on 4% (v/v) glycerol supplemented growth medium (Wu et al. 2008). Trace element solution supported growth of strain A11 by providing essential elements (Arora et al. 2016a; Jiang et al. 2020) and good microbial growth has resulted into good biosurfactant yield (Jiang et al. 2020).

### Biosurfactant characterization

Biosurfactant can be characterization is feasible by several methods like thin layer chromatography (TLC), gas chromatography (GC), Fourier transform infrared spectroscopy (FTIR), chromatography–mass spectrometry (GC–MS), electrospray ionization mass spectrometry (ESI–MS), high-performance thin layer chromatography (HP-TLC),

**Fig. 1** **a** Time course of growth and surface tension reducing ability of *Pseudomonas aeruginosa* strain A11 while growing on glycerol supplemented MSM. **b** Time course of biomass and rhamnolipids production by *Pseudomonas aeruginosa* strain A11 while growing on glycerol supplemented MSM. Growth was carried out at 30 °C with 200 rpm agitation rate. Values given are mean  $\pm$  SD of three independent experiments



high performance liquid chromatography (HPLC), liquid chromatography–mass spectrometry (LC–MS), Fast atom bombardment–mass spectrometry (FAB–MS) and nuclear magnetic resonance (NMR) (Varjani and Upasani 2017). In the present study, biosurfactant produced by strain A11 was characterized TLC, FTIR, NMR and MALDI-TOF mass spectrometry.

TLC is the simple and convenient method for biosurfactant characterization. TLC profile of the biosurfactant showed two spots with  $R_f$  value of 0.45 and 0.69, corresponding to dirhamnolipid and monorhamnolipid, respectively. Earlier studies have reported two spots on TLC profile corresponding to dirhamnolipid and monorhamnolipid (Singh and Cameotra 2013; Satpute et al. 2010; Adetunji et al. 2017). Both the spots were positive for anisaldehyde suggesting biosurfactant to be glycolipids type microbial surfactants (Satpute et al. 2010; Adetunji et al. 2017).

Glycolipid nature of biosurfactant was further confirmed by FTIR. FTIR helps in determining the functional groups and the chemical bonds present in biologically active compounds. The FTIR spectrum of biosurfactant gave major peak at  $3418\text{ cm}^{-1}$  due to the  $-\text{OH}$  stretching vibration (Fig. 2). Peaks at  $1741\text{ cm}^{-1}$ ,  $1112\text{ cm}^{-1}$  and  $1058\text{ cm}^{-1}$  were also observed and these corresponds to carbonyl stretching frequencies of ester group as well as to acid groups. The observed peaks at  $2922\text{ cm}^{-1}$ ,  $2856\text{ cm}^{-1}$  and  $1466\text{--}1388\text{ cm}^{-1}$  may be attributed to the  $\text{C}\text{--}\text{H}$   $-\text{CH}_2$  and  $-\text{CH}_3$  stretching vibrations, respectively. Peaks between  $914\text{--}980\text{ cm}^{-1}$  and  $815\text{--}848\text{ cm}^{-1}$  may be due to pyranyl-I and  $\alpha$ -pyranyl-II stretching vibrations, respectively. The FTIR profile of biosurfactant exhibited similarity to glycolipids type of biosurfactant (Leitermann et al. 2008).

Identity of biosurfactant was also evaluated by  $^1\text{H}$  and  $^{13}\text{C}$  NMR. As evident from (Fig. 3a) the proton NMR spectra exhibited triplet at  $\delta$  0.82 suggesting the presence of  $-\text{CH}_3$  in lipid chain. Broad signals at  $\delta$  1.13–1.24 is due

to the presence of  $-\text{CH}_2$  in lipid chains. Peaks at  $\delta$  2.37 may be attributed to  $-\text{CH}_2$  of the ester carbonyl and peak at  $\delta$  2.47 is due to the  $-\text{CH}_2$  attached to the acid carbonyl. Peaks from  $\delta$  3.91 to  $\delta$  3.98 exhibit the  $-\text{CH}$  protons in the rhamnose moiety. Peak at  $\delta$  4.82 indicates presence of  $-\text{CH}$  attachment to the  $-\text{O}-$  of ester moiety. The peak at  $\delta$  5.33 is due to the hydrogen on anomeric carbon while peak at  $\delta$  10.0 shows the presence of acidic proton of lipid moiety.

The  $^{13}\text{C}$  NMR spectrogram exhibited peak at  $\delta$  13.9 which is due to  $-\text{CH}_3$  in lipid chain (Fig. 3b). Peaks at  $\delta$  22.4, 24.3, 24.9, 28.9, 29.2, 29.5, 31.5, 34.2, 38.9 and 39.4 may be attributed to the  $-\text{CH}_2$  in the lipid chain. The peak at  $\delta$  64.0 may be due to the  $-\text{CH}$  attached to the O of ester moiety. The peaks between  $\delta$  68.0 and 73.1 is due to the presence of deshielded  $-\text{CH}$  in rhamnose moiety. Peaks at  $\delta$  79.2 and  $\delta$  102.4 are due to the linkage of two rhamnose moieties. The linkage of rhamnose moiety and lipid unit is demonstrated by the peak at  $\delta$  95.8. The peak at  $\delta$  171.3 and  $\delta$  173.3 confirms the presence of ester and acid in lipid unit, respectively. The  $^1\text{H}$  and  $^{13}\text{C}$  NMR spectra of biosurfactant suggested it to be rhamnolipids (Jadhav et al. 2011).

Rhamnolipids identity of biosurfactant was further confirmed by MALDI-TOF mass spectrometry. MALDI-TOF mass spectra of rhamnolipids exhibited peaks which can be assigned to the sodium and potassium adducts (Rooney et al. 2009). The results of MALDI-TOF mass spectrometric analyses revealed that both mono- and dirhamnolipid moieties are present in the rhamnolipids produced by *P. aeruginosa* strain A11 (Fig. 4). As evident from Fig. 4, most abundant rhamnolipid was observed at  $m/z$  673.26 which corresponds to dirhamnolipid ( $\text{RhaRhaC}_{10}\text{C}_{10}$ ). Most abundant monorhamnolipid congener ( $\text{RhaC}_{10}\text{C}_{10}$ ) was observed at  $m/z$  527.23. Olefinic rhamnolipids were also produced by strain A11. Table 1 shows assignment of all rhamnolipids, mass peaks and their corresponding molecular formula obtained by MALDI-TOF mass spectrometry.

A glycolipid type biosurfactant is characterized by a carbohydrate moiety which act as the hydrophilic head and a fatty acid moiety constituting the hydrophobic chain. In rhamnolipids, the carbohydrate moiety is constituted by L-rhamnose sugar (Muller et al. 2012). Fatty acid moiety is linked to rhamnose sugar by glycosidic bond. Earlier study had shown that rhamnolipids obtained from strain A11 consisted of seven dirhamnolipids congener and single monorhamnolipids congener (Singh and Cameotra 2013). Contrary in the present study use of sophisticated analytical method helped in identifying more homologous and congeners (Abdel et al. 2010).

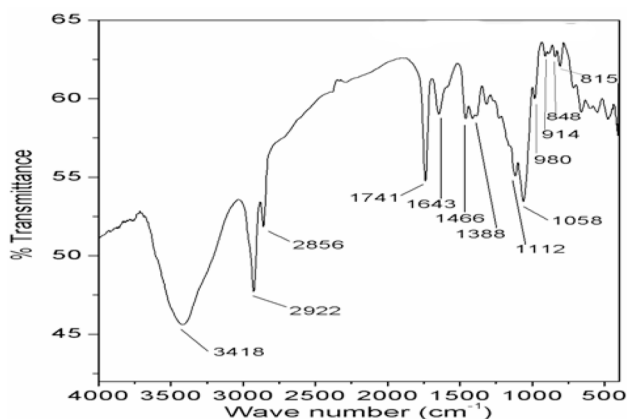
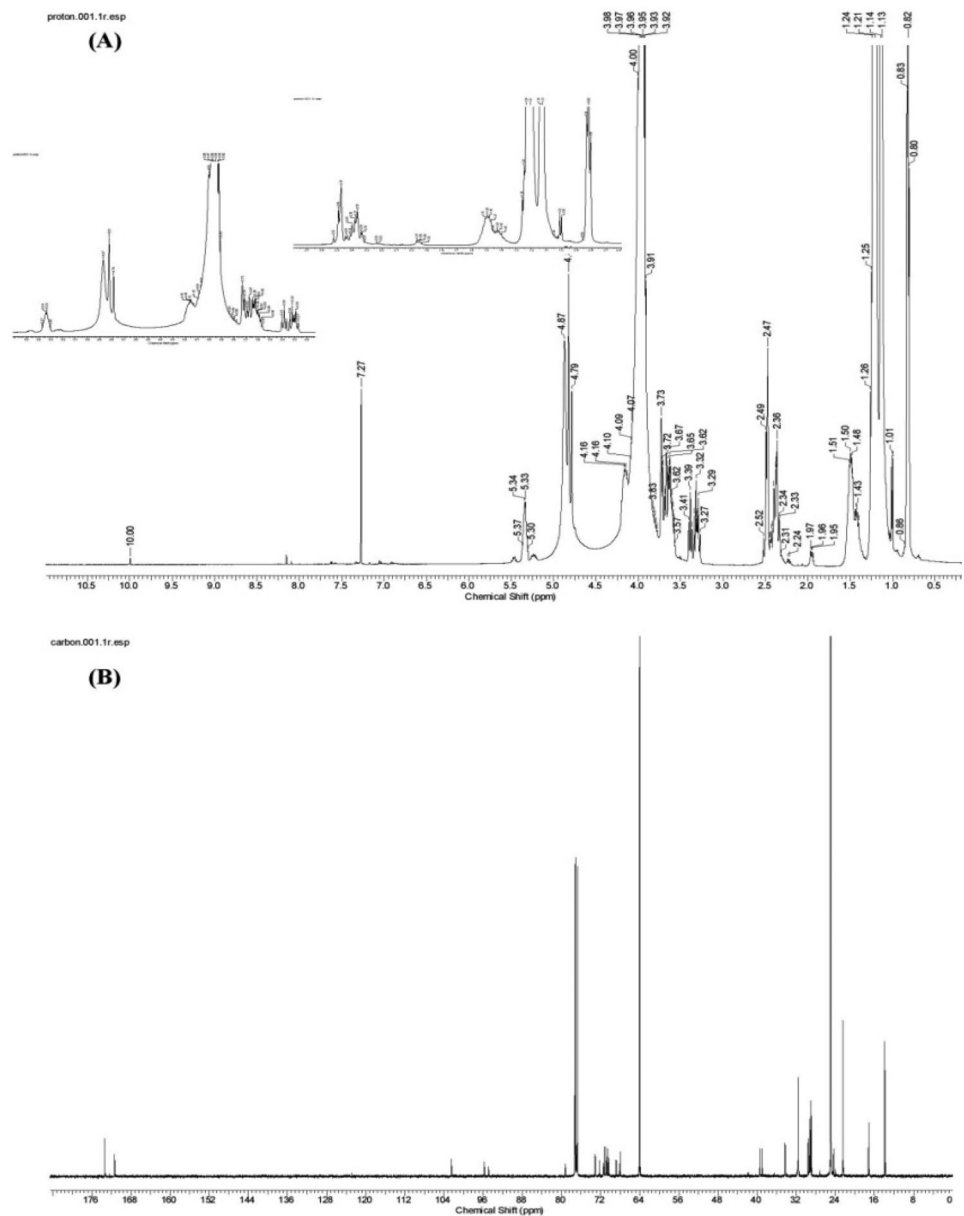


**Fig. 2** FTIR spectrum of biosurfactant produced by *Pseudomonas aeruginosa* strain A11

**Fig. 3** NMR spectra of purified rhamnolipids **a**  $^1\text{H}$  spectra **b**  $^{13}\text{C}$  spectra



### Surface tension reducing activity and critical micelle concentration (CMC)

Surface tension reducing ability and CMC of biosurfactant are important physical properties which impact its applications, commercial value as well as demand (Arora et al. 2016a). Surfactant with good surface tension reducing capability and low CMC are considered suitable for several industrial processes.

Biosurfactant obtained from strain A11 reduced surface tension of water from 72 to 36 mN/m. The CMC of biosurfactant was determined by plotting surface tension value as a function of surfactant concentration. It was observed that surface tension of water gradually decreased with increase

in biosurfactant concentration. This observation can be explained on the basis of increased accumulation of biosurfactant monomer at the water–gas inter-phase. Once the gas–water inter-phase get saturated with monomers, biosurfactant starts entering the bulk phase of water to form micelles. Bulk water containing biosurfactant micelles shows no further decrease in surface tension upon surfactant addition and this concentration of biosurfactant is considered as critical micelle concentration. Biosurfactant obtained from strain A11 demonstrated CMC of 70 mg/l. Generally, CMC of rhamnolipids vary in the range of 53–230 mg/l depending upon rhamnolipids species composition (Abdel et al. 2010). Earlier, Singh and Cameotra (2013) observed that rhamnolipids produced by strain A11 can reduce the

**Fig. 4** MALDI-TOF mass spectra of rhamnolipids produced by *P. aeruginosa* strain A11. *Inset* Molecular structure of most abundant rhamnolipids congener

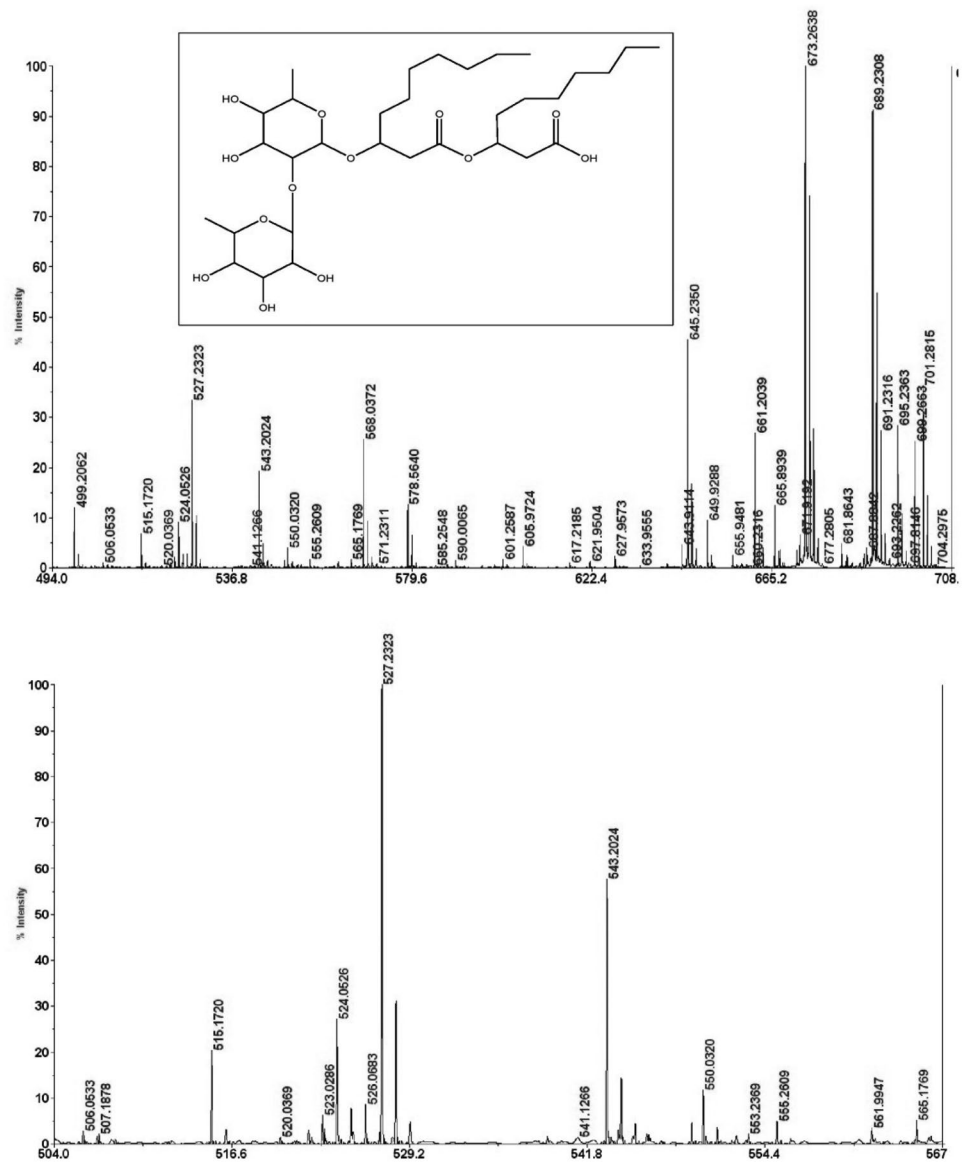


**Table 1** Assignment of all rhamnolipids mass peaks obtained by MALDI-TOF mass spectrometry

Mass peak	Assignment	Molecular formula
499.20 515.17	RhaC <sub>10</sub> C <sub>8</sub> /RhaC <sub>8</sub> C <sub>10</sub> [M + Na] <sup>+</sup> RhaC <sub>10</sub> C <sub>8</sub> /RhaC <sub>8</sub> C <sub>10</sub> [M + K] <sup>+</sup>	C <sub>22</sub> H <sub>44</sub> O <sub>9</sub>
523.02	*RhaC <sub>22</sub> [M + Na] <sup>+</sup>	C <sub>28</sub> H <sub>52</sub> O <sub>7</sub>
527.23543.20	RhaC <sub>10</sub> C <sub>10</sub> [M + Na] <sup>+</sup> RhaC <sub>10</sub> C <sub>10</sub> [M + K] <sup>+</sup>	C <sub>26</sub> H <sub>48</sub> O <sub>9</sub>
553.23	*RhaC <sub>12</sub> C <sub>10</sub> / RhaC <sub>10</sub> C <sub>12</sub> [M + Na] <sup>+</sup>	C <sub>28</sub> H <sub>50</sub> O <sub>9</sub>
555.26 571.23	RhaC <sub>12</sub> C <sub>10</sub> /RhaC <sub>10</sub> C <sub>12</sub> [M + Na] <sup>+</sup> RhaC <sub>12</sub> C <sub>10</sub> / RhaC <sub>10</sub> C <sub>12</sub> [K + Na] <sup>+</sup>	C <sub>28</sub> H <sub>52</sub> O <sub>9</sub>
645.23661.20	RhaRhaC <sub>10</sub> C <sub>8</sub> /RhaRhaC <sub>8</sub> C <sub>10</sub> [M + Na] <sup>+</sup> RhaRhaC <sub>10</sub> C <sub>8</sub> /RhaRhaC <sub>8</sub> C <sub>10</sub> [M + K] <sup>+</sup>	C <sub>30</sub> H <sub>54</sub> O <sub>13</sub>
671.91687.88	*RhaRhaC <sub>10</sub> C <sub>10</sub> [M + Na] <sup>+</sup> *RhaRhaC <sub>10</sub> C <sub>10</sub> [M + K] <sup>+</sup>	C <sub>32</sub> H <sub>56</sub> O <sub>13</sub>
673.26689.23	RhaRhaC <sub>10</sub> C <sub>10</sub> [M + Na] <sup>+</sup> RhaRhaC <sub>10</sub> C <sub>10</sub> [M + K] <sup>+</sup>	C <sub>32</sub> H <sub>58</sub> O <sub>13</sub>
699	*RhaRhaC <sub>12</sub> C <sub>10</sub> /RhaRhaC <sub>10</sub> C <sub>12</sub> [M + Na] <sup>+</sup>	C <sub>34</sub> H <sub>60</sub> O <sub>13</sub>
701.28	RhaRhaC <sub>12</sub> C <sub>10</sub> /RhaRhaC <sub>10</sub> C <sub>12</sub> [M + Na] <sup>+</sup>	C <sub>34</sub> H <sub>62</sub> O <sub>13</sub>

\*Olefinicrhamnolipid

surface tension of water to 29 mN/m with CMC of 83 mg/l (Singh and Cameotra 2013). Variation in rhamnolipids composition is known to alter surface tension reducing capability as well as CMC of biosurfactant (Singh and Cameotra 2013; Arora et al. 2016a).

### Induction time of methane hydrate kinetics

The induction time for methane hydrate formation is an important kinetic parameter. Lower induction time is desirable for the storage and transportation of gas through hydrate form (Linga et al. 2012). The induction time of gas hydrate formation gives indication of the nucleation period in which water and gas molecules are in the metastable region interact to make nuclei of a critical size leading to growth of gas hydrates (Sloan 1998). Usually, induction time is indicated by a sudden fall in the pressure and simultaneous sharp rise in temperature.

The effect of rhamnolipids at different concentrations on the induction time was investigated in porous system consisting of C type silica gel. Figure 5 shows variation in pressure and temperature with respect to time during methane hydrate formation process. As evident from Fig. 5a and b, initially there was a simultaneous decrease in pressure and temperature due to the gas contraction and dissolution in the aqueous phase. At hydrate formation point, there was a sudden drop in pressure and a rise in temperature at the same time. This rise in temperature is due to the release of the latent heat of hydrate formation. The induction time was reported as the difference between time of start of experiment and time of hydrate nucleation. As it is evident by comparing Figs. 5a and b induction time for combination of rhamnolipids with silica gel has reduced significantly with respect to quiescent water system i.e. upto 81% and thus, exhibiting that rhamnolipids in combination with silica gel shortened induction time (Arora et al. 2016a, b; Jadav et al. 2017; Rogers et al. 2003) for methane hydrate formation.

The induction time for hydrate nucleation in a quiescent system is governed by super-saturation. The existence of additives and foreign particles decreases interfacial tension of hydrate-liquid (Carvajal-Ortiz and Pratt 2013). Chemical additives and support systems have been reported to shorten the induction time (Zhong and Rogers 2000; Saw et al. 2014; Linga et al. 2012; Kumar et al. 2016). The C type silica gel having mesh size of 230–400 has been reported to perform better than A type and B type silica gel (60–120 and 100–200 mesh, respectively) for carbon dioxide clathrate formation (Kumar et al. 2013). The C type of silica gel has higher specific area with smaller particle size which supports higher rate of hydrate formation by decreasing the induction time (Kumar et al. 2013). In a porous matrix like silica gel formation of gas hydrates takes place within the pores as well as in interstitial sites

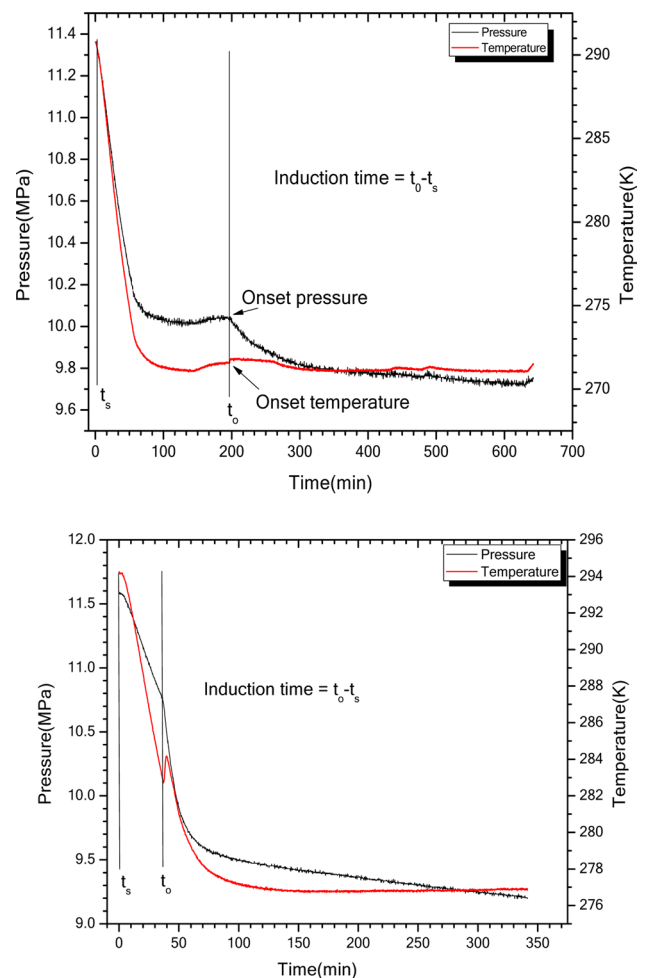


**Fig. 5** a Temperature pressure response with respect to time during methane hydrate formation in Quiescent water system. b Temperature pressure response with respect to time during methane hydrate formation in 100 ppm rhamnolipids solution saturated C type of silica gel system

(Kumar et al. 2013). Further, application of biosurfactant solution decreased interfacial tension between gas–liquid and thus, favoring better interfacial interaction between gas and water (Wang et al. 2012). The induction time gets reduced with decreasing interfacial tension of hydrate-liquid (Wang et al. 2012). Chemical additives of biological origin like rhamnolipids (Arora et al. 2016a; Jadav et al. 2017; Rogers et al. 2003) surfactin (Jadav et al. 2017; Rogers et al. 2003) lignosulfonates (Wang et al. 2012) have been reported to shorten the induction time. Rogers et al. (2003) observed 58% reduction in induction time under influence of 1000 ppm rhamnolipids (Rogers et al. 2003). Jadav et al. (2017) reported that addition of 1000 ppm of rhamnolipids to water decreased induction time of methane hydrate formation from 5.77 to 0.06 h (Jadav et al. 2017).



## Moles of gas consumed

During methane hydrate formation, methane is trapped into the cages like lattice structure of water molecule. Determining the amount of methane getting trapped during methane hydrate formation is important for gas storage. Methane hydrate formation was accompanied by increase in the moles of methane consumed and subsequent decrease in the pressure. The number of moles of methane consumed while hydrate formation have been used to calculate the rate constant of Hydrate Formation which is used to calculate methane hydrate formation rate and it was found that there is a increase of 3.2 folds for methane hydrate formation rate in presence of 1000 ppm Rhamnolipids in combination with silica gel in comparison to quiescent water system and thus exhibiting that rhamnolipids (Arora et al. 2016a, b; Jadav et al. 2017; Rogers et al. 2003) has enhanced the rate of hydrate formation.

Rapid increase in methane consumption was observed in C type of silica gel saturated with 1000 ppm rhamnolipids solution whereas most slow methane consumption was observed in the quiescent water system. Thus, suggesting that rhamnolipids in combination with C type silica gel enhanced the rate of methane hydrate formation as compared to quiescent water system and water saturated C type silica gel. The solubilisation of biosurfactant in water favors super saturation of gas molecules in a solution. This results in accelerated mass transfer from bulk phase to hydrates and thus, increasing the moles of methane consumed during hydrate formation.

The number of moles of methane consumed in the presence of rhamnolipids is more than its synthetic counter parts (nonylphenolethoxalate quaternary ammonium salt and linear alkyl benzene sulfonic acid) (Karaaslan and Parlaktuna 2000). Carvajal-Ortiz and Pratt (2013) reported that overall methane consumption was more in biosurfactant and biosurfactant–smectite experiment system than smectite–clay experiments (Carvajal-Ortiz and Pratt 2013). Zhong and Rogers (2000) reported that there is more ethane consumption when hydrates were formed from solutions containing 284 ppm synthetic surfactant SDS.

## Water to hydrate conversion

The percentage of water to hydrate conversion is the number of water moles converted into hydrate per moles of water. The percentage of water to hydrate conversion till 237.5 min is given in Fig. 6. At a given time the percentage of water to hydrate conversion is found to be better in the presence of 1000 ppm rhamnolipid. The percentage of water to hydrate conversion till the end of the reaction for quiescent water system, water saturated C type silica gel and 1000 ppm rhamnolipids saturated silica gel was observed to be 8.43%

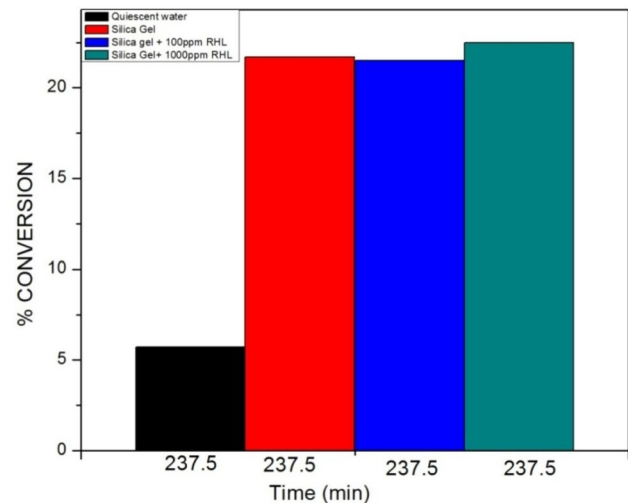


Fig. 6 Percentage water to hydrate conversion

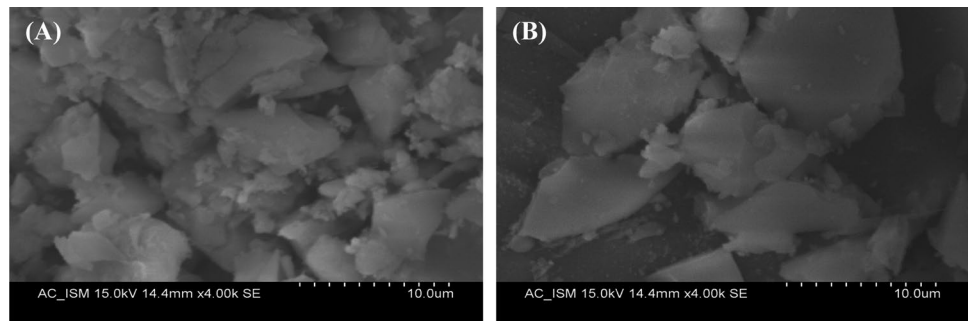
(642.1 min), 22.2% (363.0 min), and 22.5% (237.5 min), respectively. The silica gel used in this work shows far better water to hydrate conversion rate which was further improved in the presence of rhamnolipids. Conversion reported by Zhang et al. (2013) in the presence of silica gel powder is around 8% till 5 h (Zhang et al. 2013). Jadav et al. (2017) reported 47.3% and 45.1% conversion of methane to hydrate in the presence of 200 ppm rhamnolipids and water without rhamnolipids respectively (Jadav et al. 2017).

In quiescent water system, gas hydrates start to crystallize at the gas–liquid interface and not in the bulk phase of water. Nucleation and growth takes place in the form of thin film at the gas–liquid interface. This result in slow hydrate formation in a quiescent water system as thin film of hydrate present at the water surface prevents mass transfer across the film subsequently slowing kinetics and lowering water to hydrate conversion (Kumar et al. 2013). In the presence of surfactant, the obstructing hydrate film formation does not take place (Carvajal-Ortiz and Pratt 2013; Kumar et al. 2013). The key function of a hydrate promoting agent is to increase the solubility of the hydrate forming gas in water. Use of surfactant above the CMC increases the solubility of hydrate forming gas while at the surfactant concentration below or at CMC, gas solubility remain nearly same as that of pure water. Thus, surfactant can act as a kinetic promoter of gas hydrate only at concentrations above CMC.

## SEM analysis of silica

SEM of silica gel helped in visualizing the morphological changes induced upon methane hydrate formation. Morphologically silica particles were smooth irregular and non-porous (Fig. 7a). The irregular nature of silica provide better contact area between methane and liquid phase as compared

**Fig. 7** Scanning electron micrograph of silica gel **a** before and **b** after methane gas hydrate formation



to the gas–liquid interface prevalent in stirred reactor. Better contact area favors faster nucleation and consequently, enhanced hydrates growth. After methane hydrate formation the silica particles were observed to be swollen (Fig. 7b). This may be due to the methane hydrate formation in the pores of silica that led to larger inter-particle separation and therefore, slightly higher silica porosity.

So the above study has revealed that Rhamnolipids in combination with silica gel act as a promoter for methane hydrate formation which can be considered as potential hydrate promoter, hence it can replace the usage of synthetic surfactants. Hydrates despite of future generation fuel are finding many novel applications these days such as hydrate based Carbon Capture, Storage as well as transportation of natural gas etc. (Arora et al. 2015a, b; Vedachalam et al. 2020; Saw et al. 2014; Choudhary et al. 2019).

## Conclusions

The present study reports effect of rhamnolipids produced by *P. aeruginosa* strain A11 on induction time, moles of methane consumed and percentage water to hydrate conversion during methane hydrate formation. Rhamnolipids produced by *P. aeruginosa* strain A11 was characterized as mixture of mixture of congeners and homologues. Dirhamnolipids (RhaRhaC<sub>10</sub>C<sub>10</sub>) is the most dominating rhamnolipids congener. The gas hydrates formation experiments exhibited that saturating C type silica gel by 100 ppm rhamnolipids solution reduced the induction time, increased moles of methane consumed and enhanced water to hydrate conversion. Results suggest that combination of rhamnolipids and C type silica gel can be used as environment friendly kinetic promoter in methane hydrate formation process.

**Supplementary Information** The online version contains supplementary material available at <https://doi.org/10.1007/s11001-020-09426-6>.

**Acknowledgements** The support provided by sending Amit Arora on study leave from Shaheed Bhagat Singh State Technical Campus Ferozepur to Indian Institute of Technology Roorkee is highly acknowledged. The support from institutes namely Indian Institute of Technology Roorkee Roorkee India National Chemical Laboratory (CSIR) Maharashtra Pune India, Institute of Microbial Technology (CSIR) UT Chandigarh India Keshav Dev Malviya Institute of Petroleum Exploration Oil and Natural Gas Corporation (ONGC) Utrakhnad Dehradun India Gas Hydrate Research & Technology Centre Oil and Natural Gas Corporation Ltd (ONGC) ONGC Complex Phase-II Panvel Navi Mumbai India Indian Institute of Technology (Indian School of Mines) Jharkhand Dhanbad India Indian Institute of Technology Madras Chennai is highly acknowledged.

## References

- Abdel MAM, Lepine F, Deziel E (2010) Rhamnolipids: diversity of structures microbial origins and roles. *Appl Microbiol Biotechnol* 86:1323–1336. <https://doi.org/10.1007/s00253-010-2498-2>
- Abedi-Farizhendi S, Iranshahi M, Mohammadi A, Manteghian M, Mohammadi HA (2019) Kinetic study of methane hydrate formation in the presence of carbon nanostructures. *Pet Sci* 16:657–668. <https://doi.org/10.1007/s12182-019-0327-5>
- Adetunji C, Oloke J, Mishra P, Singh RJ, Singh AK, Cameotra SS, Micheal BO (2017) Characterization and optimization of a rhamnolipid from *Pseudomonas aeruginosa* C1501 with novel biosurfactant activities. *Sustain Chem Pharm* 6:26–36. <https://doi.org/10.1016/j.scp.2017.07.001>
- Arora A, Cameotra SS, Kumar R, Kumar P, Balomajumder C (2014) Effects of biosurfactants on gas hydrates. *J Pet Environ Biotechnol* 5(2):170. <https://doi.org/10.4172/2157-7463.1000170>
- Arora A, Cameotra SS, Balomajumder C (2015a) Natural gas hydrate (clathrates) as an untapped resource of natural gas. *J Pet Environ Biotechnol* 6(4):234. <https://doi.org/10.4172/2157-7463.1000234>
- Arora A, Cameotra SS, Balomajumder C (2015b) Natural gas hydrate as an upcoming resource of energy. *J Pet Environ Biotechnol* 6(1):199. <https://doi.org/10.4172/2157-7463.1000199>
- Arora A, Cameotra SS, Kumar R, Balomajumder C, Singh AK, Santhakumari B, Kumar P, Laik S (2016a) Biosurfactant as a promoter of methane hydrate formation: thermodynamic and kinetic studies. *Sci Rep* 6:20893. <https://doi.org/10.1038/srep20893>
- Arora A, Cameotra SS, Kumar R, Singh AK, Kumar P, Balomajumder C, Laik S (2016b) Role of rhamnolipid a bio-surfactant in methane hydrate formation kinetics. *Proceedings of the first international conference on recent advances in bioenergy research*. Springer Proceedings in Energy, pp 333–343. [https://doi.org/10.1007/978-81-322-2773-1\\_25](https://doi.org/10.1007/978-81-322-2773-1_25).

- Carvajal-Ortiz H, Pratt LM (2013) Effects of clay minerals and biosurfactants on isotopic and molecular characteristics of methane encaged in pressure vessel gas hydrates. *Org Geochem* 60:83–92. <https://doi.org/10.1155/2010/271291>
- Chaturvedi E, Prasad N, Mandal A (2018) Enhanced formation of methane hydrate using a novel synthesized anionic surfactant for application in storage and transportation of natural gas. *J Nat Gas Sci Eng* 56:246–257. <https://doi.org/10.1016/j.jngse.2018.06.016>
- Chong ZR, Yang SHB, Babu P, Linga P, Li X-S (2016) Review of natural gas hydrates as an energy resource: prospects and challenges. *Appl Energy* 162:1633–1652. <https://doi.org/10.1016/j.apenergy.2014.12.061>
- Choudhary N, Chakrabarty S, Roy S, Kumar R (2019) A comparison of different water models for melting point calculation of methane hydrate using molecular dynamics simulations. *Chem Phys* 516:6–14. <https://doi.org/10.1016/j.chemphys.2018.08.036>
- Hester KC, Brewer PG (2009) Clathrate hydrates in nature. *Annu Rev Mar Sci* 1:303–327. <https://doi.org/10.1146/annurev.marine.010908.163824>
- Heydari A, Peyvandi K (2019) Role of metallic porous media and surfactant on kinetics of methane hydrate formation and capacity of gas storage. *J Pet Sci Eng* 181:106235. <https://doi.org/10.1016/j.petrol.2019.106235>
- Jiang J, Zu Y, Li X, Meng Q, Long X (2020) Recent progress towards industrial rhamnolipids fermentation: process optimization and foam control. *Bioresour Technol* 298:122394. <https://doi.org/10.1016/j.biortech.2019.122394>
- Jadhav M, Kalme S, Tamboli D, Govindwar S (2011) Rhamnolipid from *Pseudomonas desmolyticum* NCIM-2112 and its role in the degradation of Brown 3REL. *J Basic Microbiol* 51:385–396. <https://doi.org/10.1002/jobm.201000364>
- Jadav S, Sakthipriya N, Doble M, Sangwai JS (2017) Effect of biosurfactants produced by *Bacillus subtilis* and *Pseudomonas aeruginosa* on the formation kinetics of methane hydrates. *J Nat Gas Sci Eng* 43:156–166. <https://doi.org/10.1021/ie070627r>
- Karaaslan U, Parlaktuna M (2000) Surfactants as hydrate promoters? *Energy Fuels* 14:1103–1107. <https://doi.org/10.1021/ef000069s>
- Kumar A, Sakpal T, Linga P, Kumar R (2013) Influence of contact medium and surfactants on carbon dioxide clathrate hydrate kinetics. *Fuel* 105:664–671. <https://doi.org/10.1016/j.fuel.2012.10.031>
- Kumar SV, Udayabhanu G, Mandal A, Laik S (2016) Methane hydrate formation and dissociation in the presence of silica sand and bentonite clay. *Oil Gas Sci Technol Rev IFP Energies Nouvelles* 70(6):1087–1099. <https://doi.org/10.1038/srep20893>
- Leitermann F, Syldatk C, Hausmann R (2008) Fast quantitative determination of microbial rhamnolipids from cultivation broths by ATR-FTIR spectroscopy. *J Biol Eng* 2(1):13. <https://doi.org/10.1186/1754-1611-2-13>
- Linga P, Kumar R, Lee JD, Ripmeester J, Englezos P (2010) A new apparatus to enhance the rate of gas hydrate formation: application to capture of carbon dioxide. *Int J Greenh Gas Control* 4:630–637. <https://doi.org/10.1016/j.egypro.2017.03.867>
- Linga P, Daraboina N, Ripmeester JA, Englezos P (2012) Enhanced rate of gas hydrate formation in a fixed bed column filled with sand compared to a stirred vessel. *Chem Eng Sci* 68:617–623. <https://doi.org/10.1016/j.egypro.2017.03.867>
- Meleshkin AV, Bartashevich MV, Glezer VV, Glebov RA (2020) Effect of surfactants on synthesis of gas hydrates. *J Eng Thermophys* 29:264–266. <https://doi.org/10.1134/S1810232820020083>
- Muller MM, Kugler JH, Henkel M, Gerlitzki M, Hormann B, Pohnlein M, Syldatk C, Hausmann R (2012) Rhamnolipids—next generation surfactants? *J Biotechnol* 162(4):366–380. <https://doi.org/10.1016/j.jbiotec.2012.05.022>
- Rogers RE, Kothapalli C, Lee MS, Woolsey JR (2003) Catalysis of gas hydrates by biosurfactants in seawater-saturated sand/clay. *Can J Chem Eng* 81:973–980. <https://doi.org/10.1002/cjce.5450810508>
- Rooney AP, Price NP, Ray KJ, Kuo TM (2009) Isolation and characterization of rhamnolipid-producing bacterial strains from a biodiesel facility. *FEMS Microbiol Lett* 295:82–87. <https://doi.org/10.1111/j.1574-6968.2009.01581.x>
- Ruffine L, Donval JP, Charlou JL, Cremre A, Zehnder BH (2010) Experimental study of gas hydrate formation and destabilisation using a novel high-pressure apparatus. *Mar Petrol Geol* 27:1157–1165. <https://doi.org/10.1016/j.marpetgeo.2010.03.002>
- Satpute SK, Banpurkar AG, Dhakephalkar PK, Banat IM, Chopade BA (2010) Methods for investigating biosurfactants and bioemulsifiers: a review. *Crit Rev Biotechnol* 30(2):127–144. <https://doi.org/10.3109/07388550903427280>
- Saw VK, Gudala M, Udayabhanu G, Mandal A, Laik S (2014) Kinetics of methane hydrate formation and its dissociation in presence of non-ionic surfactant Tergitol. *J Unconv Oil Gas Resour* 6:54–59. <https://doi.org/10.1016/j.juogr.2013.07.001>
- Singh AK, Cameotra SS (2013) Rhamnolipids production by multi-metal-resistant and plant-growth-promoting rhizobacteria. *Appl Biochem Biotechnol* 170:1038–1056. <https://doi.org/10.1007/s12010-013-0244-9>
- Sloan ED (1998) Gas hydrates: review of physical/chemical properties. *Energy Fuels* 12:191–196. <https://doi.org/10.1021/ef970164+>
- Sloan ED, Koh CA (2008) Clathrate hydrates of natural gases, 3rd edn. CRC Press, Taylor & Francis Group, Boca Raton
- Sun F, Chen H (2008) Organosolv pretreatment by crude glycerol from oleochemicals industry for enzymatic hydrolysis of wheat straw. *Bioresour Technol* 99:5474–5479. <https://doi.org/10.1016/j.biortech.2007.11.001>
- Varjani SJ, Upasani VN (2017) Critical review on biosurfactant analysis, purification and characterization using rhamnolipid as a model biosurfactant. *Bioresour Technol* 232:389–397. <https://doi.org/10.1016/j.biortech.2019.122394>
- Vedachalam N, Ramesh S, Jyothi VBN, Ramadass GA, Atmanand MA, Manivannan P (2020) Techno-economic viability studies on methane gas production from gas hydrates reservoir in the Krishna-Godavari basin, east coast of India. *J Nat Gas Sci Eng* 77:103253. <https://doi.org/10.1016/j.jngse.2020.103253>
- Wang W, Huang Z, Chen H, Tan Z, Chen C, Sun L (2012) Methane hydrates with a high capacity and a high formation rate promoted by biosurfactants. *Chem Commun* 48:11638–11640. <https://doi.org/10.1039/C2CC35603A>
- Wu JY, Yeh KL, Lu WB, Lin CL, Chang JS (2008) Rhamnolipid production with indigenous *Pseudomonas aeruginosa* EM1 isolated from oil-contaminated site. *Bioresour Technol* 99:1157–1164. <https://doi.org/10.1016/j.biortech.2007.02.026>
- Zhang ZG, Wang Y, Gao LF, Zhang Y, Liu CS (2012) Marine gas hydrates: future energy or environmental killer? *Energy Procedia* 16:933–938. <https://doi.org/10.1016/j.egypro.2012.01.149>
- Zhang P, Wu Q, Yang Y (2013) Characteristics of methane hydrate formation in artificial and natural media. *Energies* 6:1233–1249. <https://doi.org/10.3390/en6031233>
- Zhang Z, Liu Z, Pan Z, Baena-Moreno FM, Soltanian MR (2020) Effect of porous media and its distribution on methane hydrate formation in the presence of surfactant. *Appl Energy* 261:114373. <https://doi.org/10.1016/j.apenergy.2019.114373>
- Zhong Y, Rogers RE (2000) Surfactant effects on gas hydrate formation. *Chem Eng Sci* 55:4175–4187. [https://doi.org/10.1016/S1004-9541\(08\)60287-6](https://doi.org/10.1016/S1004-9541(08)60287-6)